


**POLİTEKNİK DERGİSİ**

***JOURNAL of POLYTECHNIC***

ISSN: 1302-0900 (PRINT), ISSN: 2147-9429 (ONLINE)

URL: http://dergipark.org.tr/politeknik

CLARIVATE ANALYTICS
EMERGING SOURCES CITATION INDEX
INDEXED

# Digital image watermarking with hybrid structure of DWT, DCT, SVD techniques and the optimization with BFO algorithm

## *DWT, DCT, SVD tekniklerinden oluşan hibrid yapı ile dijital görüntü filigran ekleme ve BFO algoritması ile optimizasyonu*

***Yazar(lar) (Author(s))**: Sadik YILDIZ[1], Furkan ÜSTÜNSOY[2], H. Hüseyin SAYAN[3]*

*ORCID[1]: 0000-0003-4733-4684*

*ORCID[2]: 0000-0003-3087-895X*

*ORCID[3]: 0000-0002-0692-172X*

ERKEN GÖRÜNÜM

**To cite to this article**: Yıldız S., Üstünsoy F., and Sayan H. H., "Digital Image Watermarking with Hybrid Structure of DWT, DCT, SVD Techniques and The Optimization with BFO Algorithm", ***Journal of Polytechnic***, *(*): *, (*).

**Bu makaleye şu şekilde atıfta bulunabilirsiniz:** Yıldız S., Üstünsoy F., and Sayan H. H., "Digital Image Watermarking with Hybrid Structure of DWT, DCT, SVD Techniques and The Optimization with BFO Algorithm", ***Politeknik Dergisi***, *(*): *, (*).

**Erişim linki (To link to this article):** http://dergipark.org.tr/politeknik/archive

**DOI:** 10.2339/politeknik.1192824

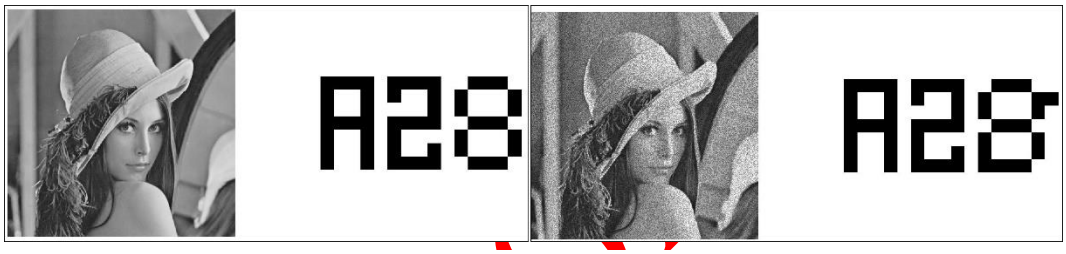
# Digital Image Watermarking with Hybrid Structure of DWT, DCT, SVD Techniques and The Optimization with BFO Algorithm

## *Highlights*

- *A hybrid watermarking method has been applied by using DWT, DCT and SVD, which are among the watermarking methods used to prevent copyright violations and privacy violations in digital images.*
- *"Gaussian", "shot", "salt & pepper" and "speckle" noises are added to watermarked images, respectively.*
- *The original image and the watermark have been extracted from the watermarked image after adding noise.*
- *The original image and watermark have been re-extracted from the optimized watermarked image by using the BFO technique. In this step, PSO algorithm has been used to set the best position of the chemotactic parameters of the BFO algorithm.*
- *PSNR, NCC and IF values have been calculated and compared to see the success performance of watermarking techniques and optimization techniques.*

## *Graphical Abstract*

*It has been observed that the applied hybrid structure with DWT, DCT, SVD and optimization techniques BFO and PSO give successful results in embedding and extraction watermarks.*



**(a)** **(b)**

**Figure.** a) Original image and watermark b) After DWT-DCT-SVD-PBFO hybrid technique, watermarked image and extracted watermark

## *Aim*

*The aim is to show the success of the hybrid structure consisting of DWT, DCT and SVD which are the methods of embedding watermarks for preserving digital images and to increase the success of the hybrid structure by using the optimization methods BFO and PSO.*

## *Design & Methodology*

*MATLAB R2020b program was used for experimental studies. All watermarking and optimization process have been executed with MATLAB editor.*

## *Originality*

*The watermark embedding and extraction methods DWT, DCT, SVD and the optimization algorithms BFO and PSO were used together.*

## *Findings*

*Experimental results have been shows that hybrid watermarking methods and optimization methods together gives successful results.*

## *Conclusion*

*It has been observed that the applied hybrid structure and optimization techniques give successful results in embedding and extraction watermarks.*

## *Declaration of Ethical Standards*

*The author(s) of this article declare that the materials and methods used in this study do not require ethical committee permission and/or legal-special permission.*

# Digital Image Watermarking with Hybrid Structure of DWT, DCT, SVD Techniques and The Optimization with BFO Algorithm

*Araştırma Makalesi / Research Article*

**Sadık Yıldız[1*], Furkan Üstünsoy[2], H. Hüseyin Sayan[3]**
[1,2]Institute of Natural and Applied Sciences, Gazi University, Turkey
[3]Faculty of Technology, Electrical Electronic Engineering Department, Gazi University, Turkey
(Geliş/Received : 21.10.2022 ; Kabul/Accepted : 18.12.2022 ; Erken Görünüm/Early View : 31.01.2023)

**ABSTRACT**

The copyright violations in digital images and the violations of the privacy of personal data are happened with the development of technology and the widespread use of the internet. The usage of watermarks in digital images provides high protection to image owners in copyright protection and in protection of personal data. In this paper, watermarks have been added to digital images by using discrete wavelet transform (DWT), discrete cosine transform (DCT) and singular value decomposition (SVD) methods, respectively. "Gaussian", "shot", "salt & pepper" and "speckle" noises are added to watermarked images, respectively. The original image and the watermark have been extracted from the watermarked image after adding noise. The original image and watermark have been re-extracted from the optimized watermarked image by using the bacterial foraging optimization (BFO) technique. In this step, the particle swarm optimization (PSO) algorithm has been used to set the best position of the chemotactic parameters of the BFO algorithm. The peak signal to noise ratio (PSNR), normalized cross correlation (NCC) and image fidelity (IF) values have been calculated and compared to see the success performance of watermarking techniques and optimization techniques.
**Keyword: Watermarking, image cryptography, metaheuristic optimization.**

# DWT, DCT, SVD Tekniklerinden oluşan Hibrid Yapı ile Dijital Görüntü Filigran Ekleme ve BFO Algoritması ile Optimizasyonu

**ÖZ**

Teknolojinin gelişmesi ve internet kullanımının yaygınlaşması ile sayısal görüntülerde telif hakkı ihlalleri ve kişisel verilerin gizliliğinde ihlaller yaşanmaktadır. Dijital görüntülerde filigran kullanmak telif haklarının korunmasında ve kişisel verilerin korunmasında görüntü sahiplerine yüksek koruma sağlamaktadır. Bu makale çalışmasında sayısal görüntülere sırasıyla ayrık dalgacık dönüşümü (DWT), ayrık kosinüs dönüşümü (DCT) ve tekil değer ayrıştırma (SVD) yöntemleri kullanılarak filigran eklendi. Filigran eklenen görüntülere sırasıyla "Gauss", "Atış", "tuz-biber" ve "benek" gürültüleri eklenmiştir. Gürültü ekleme işlemlerinin ardından filigran uygulanan görüntüden orijinal görüntü ve filigran çıkarılmıştır. Bakteri arama optimizasyonu (BFO) tekniği kullanılarak optimize edilen filigranlı görüntüden orijinal görüntü ve filigran tekrar çıkarılmıştır. Bu adımda BFO algoritmasının kemotaktik parametrelerinin en iyi *pozisyonunu belirlemek için* parçacık sürüsü optimizasyonu (PSO) algoritması kullanılmıştır. Filigran teknikleri ve optimizasyon tekniklerinin başarı performanslarını göstermek için tepe sinyal-gürültü oranı (PSNR), Normalleştirilmiş çapraz korelasyon (NCC) ve görüntü uygunluk (IF) değerleri hesaplanarak karşılaştırılmıştır.
**Anahtar Kelimeler: Filigran Ekleme, görüntü şifreleme, meta-sezgisel optimizasyon.**

ERKEN GÖRÜNÜM

## I. INTRODUCTION

Nowadays, the use and distribution of multimedia data has become widespread due to the developments in internet technology and mobile devices. During the sharing and distribution of multimedia data, digital images can be easily reproduced and manipulated. This situation causes the copyright violations of users and the violations of privacy of personal data [1, 2, 3]. Many methods are used to protect digital images, one of them is the watermarking technique [1, 2, 4, 5]. The digital watermarking is used for data protection in multimedia types of audio, video, image and text [1, 4, 6, 7]. The digital watermarking is frequently used in medical images, forensic images, media images, communication images, etc. for purposes such as proof of data accuracy, tracking of data owners, copy protection, device control, broadcast tracking and archiving. [1, 5, 8].

In recent years, many studies have been carried out on digital watermarking. In From these studies [1], an algorithm for digital image watermarking based on automatic thresholding with hybrid watermarking designed to embed watermarks in the transformation area using both DCT and DWT is proposed. In [2], a comparative study on the use of different color systems by applying the watermarking algorithms DCT and DWT for three different color systems which are Hue-Saturation-Value (HSV) color system, Red-Green-Blue (RGB) color system and YIQ color system is presented. In [4], an intelligent algorithm based on DCT–DWT–SVD has been applied to strike a balance between

*Corresponding Author
*e-posta : sadikyildiz06@gmail.com*

imperceptibility and robustness in digital image watermarking. Simultaneously, genetic programming and PSO techniques have been used to achieve the best efficiency in robustness without losing image quality. In [5], digital watermarking which is using DWT and DCT techniques was performed to embed patient information in the medical image. In [9], an adaptive median filter and BFO have been proposed to improve the PSNR value of the highly distorted image affected by impact noise. With these techniques, salt and pepper noise of highly distorted images is eliminated up to 90%. In [6], a digital watermarking technique based on DWT, DCT and Grasshopper Optimization Algorithm (GOA) is proposed. In [7], DWT-SVD based secure sparse watermarking method is proposed for digital images. The study in [3] presents an optimized watermarking with DWT and SVD techniques. The singular values of a dual watermark are embedded in the singular values of the LL sub-band coefficients of the main image by using multiple scaling factors. In [10], a new image embedding method based on DWT, Hessenberg decomposition (HD) and SVD is proposed. Also, fruit fly algorithm was used for image optimization.

In this study, digital watermarking method has been applied to eight-bit deep gray level digital images by using DWT, DCT and SVD techniques. Noise has the effect of distorting image signals. For this reason, "gaussian", "shot", "salt & pepper" and "speckle" noises were added to the watermarked images, respectively. After adding noise, the original image and watermark have been extracted from the watermarked image. *PSNR*, *NCC* and *IF* values have been calculated and compared to show the success performance of watermark techniques. In order to increase the success rate of the watermark techniques, the original image and the watermark have been extracted from the noise-added watermarked image that has been optimized with BFO. It has been observed that the image quality has improved. In addition, the PSO algorithm has been used to set the best position of the chemotactic parameters in the BFO algorithm and its effect on image quality in watermark extraction has been investigated.

## II. SUGGESTED METHODS AND TECHNIQUES

### A- Discrete Wave Transformation

DWT is one of the common and popular mathematical conversions used for digital watermarking [2, 10, 11]. The DWT technique has the effect of effective resistance to noise and geometric operations such as clipping [10]. The image is decomposed into various resolution levels (N-Level) as in the human visual system with the DWT technique [1, 11,12]. The image is first separated into two different frequency regions by passing it through a high-pass filter when decomposing it. With this process, the image is vertically transformed into one dimensionally (1-D). Then, a 1-D transformation is applied to the image horizontally. With this process, the image is subjected to a single-level 2-D DWT process. With this last step, the image is decomposed into four different non-overlapping frequency bands. The four sub-bands from a one-step 2-D decomposition are named LL (Low-Low or cA), LH (Low-High or cH), HL (High-Low or cV), and HH (High-High or cD), respectively (Figure 1). Any of these sub-bands can be further decomposed according to the application requirement [1 ,2, 10, 11].

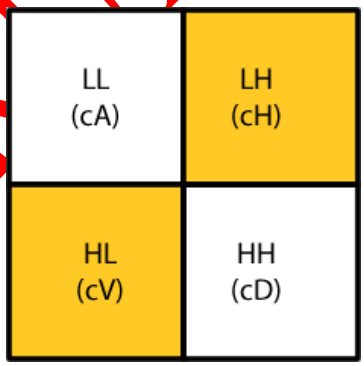



**Figure 1**- Single-level 2-D DWT Processing

DWT analysis is performed as follows (Figure 2).

$$cA + p[r,s] = (cA(r,s) * h[-r]) \downarrow 2 \qquad (1)$$

$$dA + p[r,s] = (cA(r,s) * g[-r]) \downarrow 2 \qquad (2)$$

Here, the DWT process is expressed as:

$$cA + p[r,s] = [(cA\,(r,s) \uparrow 2) * h[r]) + [(dA(r,s) \uparrow 2) * g[r])] \qquad (3)$$

Here:

*h [r]* : Low pass filter
*g [r]* : High pass filter
*h [-r]* : Low pass analysis filter
*g [-r]* : High pass analysis filter
* : Convolution
↑↓ : Up and down sampling
*cA* : High band output coefficient at level *n*
*dA* : Low band output coefficient at level *n*

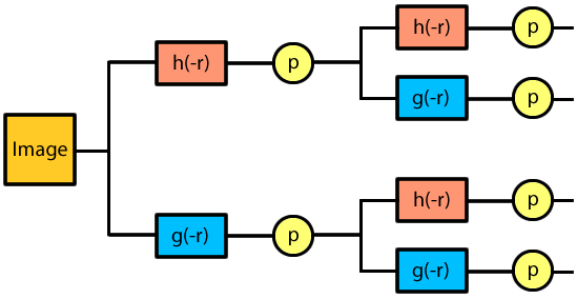



**Figure 2** – 2-D decomposition with DWT

ERKEN GÖRÜNÜM

**B- Discrete Cosine Transformation**

Due to the high compression feature of DCT, it stands out among the vertical change methods used for image editing. The DCT technique helps us to determine the most suitable area in the image in the watermark process [2]. DCT is a transformation that maps the image data to a mathematical field with its own spatial mathematical equation. In DCT technique, two-dimensional image p is taken as input and the image is moved from the spatial plane to the frequency plane (Figure 3). The carrier signal is divided into three frequency bands: high, medium and low. In this frequency-based watermark scheme, the pixels of the carrier image are not directly affected because the watermark is hidden in one of these three bands [1, 2, 4, 11, 13, 14]. The DCT equation is applied to the image pixel values in the frequency plane to match the new image coefficients with the two-dimensional mathematical matrix. The two-dimensional DCT (2D-DCT) for image p with dimensions R×S is defined as [1, 2, 13, 14]:

$$F(jk) = a_j a_k \sum_{r=0}^{R-1} \sum_{s=0}^{S-1} f(r,s) \cos\left[\frac{(2r+1)j\pi}{2R}\right] \cos\left[\frac{(2s+1)k\pi}{2S}\right] \quad (4)$$

The inverse transform formula for 2D-DCT is defined as follows,

$$f(rs) = a_j a_k \sum_{j=0}^{R-1} \sum_{k=0}^{S-1} a(j)a(k) \cos\left[\frac{(2r+1)j\pi}{2R}\right] \cos\left[\frac{(2s+1)k\pi}{2S}\right] \quad (5)$$

Here, $M$ and $N$ image sizes.

$0 \le j \le R-1, 0 \le k \le S-1$

$$a(j) = \begin{cases} \frac{1}{\sqrt{R}} & j = 0 \\ \sqrt{\frac{2}{R}}, & 1 \le j \le R-1 \end{cases}$$

$$a(k) = \begin{cases} \frac{1}{\sqrt{S}} & j = 0 \\ \sqrt{\frac{2}{S}}, & 1 \le k \le S-1 \end{cases}$$

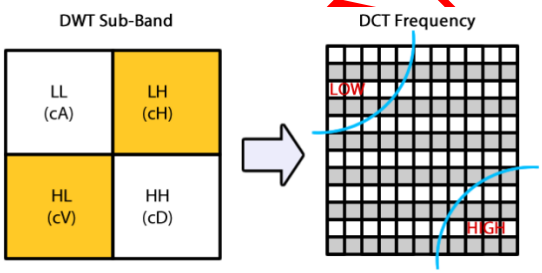



**Figure 3** - DWT Sub-Band to DCT Frequency Domain

**C- Singular Value Decomposition**

SVD is a remarkably efficient linear algebra data analysis tool for image encoding, compression, and watermarking. SVD is a linear algebra method. It is used to decomposes the matrix into three component matrices (Figure 4). If we accept the image as $r \times s$ matrix $A$, and apply SVD to matrix $A$, we will get the following equation [4, 10, 15, 16, 17].

$$A = U * S * V^T \quad (6)$$

Here;

U: Orthogonal matrix (left singular values $r \times r$)

V: Orthogonal matrix (right singular values $s \times s$)

S: Diagonal matrix (singular values $r \times s$).

Their values should increase as here;

*s (1, 1)>s (2, 2)>s (3, 3)> . . . >s (r,s)*

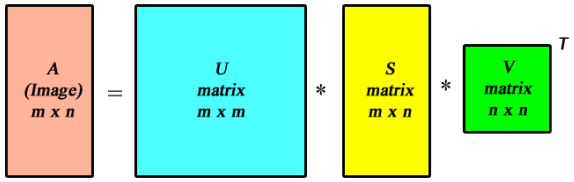



**Figure 4** – Demonstration of the SVD technique

When the watermark is embedded with SVD technique, it provides high accuracy, robustness and high imperceptibility in the resolution of the image [18].

**D- Bacterial Foraging Optimization Algorithm**

BFO algorithm is a metaheuristic optimization algorithm. The BFO technique is a calculation method to solve complex engineering problems by modeling the E. coli bacteria foraging behavior. Bacteria are much simpler than other species which are in complex life forms. They need to perform nutritional activities expending energy at the optimum level by using their limited perception and movement abilities. They are easier to model than other life forms. E. coli bacteria, which is one of such creatures, is one of the microorganisms whose structure and working style are best understood. E. Coli bacteria releases a chemical substance which stimulates other bacteria when it finds the nutrient. With the effect of this chemical substance, E. coli bacteria move towards the location of nutrient. If the nutrient density is too high, the bacteria can move as a group by clamping down. When E. coli bacterial cells search for nutrient, they perform chemotaxis (swimming and rolling), swarming, reproduction, elimination and dispersal activities. While the flagella and the base of the flagellum rotate counterclockwise, Chemotaxis is a left-handed helix structured to generate force against the bacteria and repel

ERKEN GÖRÜNÜM

the cell. Otherwise, each flagellum moves independently and rolls clockwise (Figure 5) [9, 19, 20, 21].

BFO algorithm consists of four stages [9, 22];

**1- Chemotaxis**: At this stage, the foraging movement of an E. coli cell is modeled. The E. coli cell foraging with swimming and rolling movement by using its flagella. It can roll or swim in the opposite direction. It moves with these two actions throughout its life. Bacteria rolling more frequently in areas where food is poorer while they swim in areas where food is more abundant. Figure 5 shows how a bacterium moves clockwise and counterclockwise in a nutrient solution [20, 21].

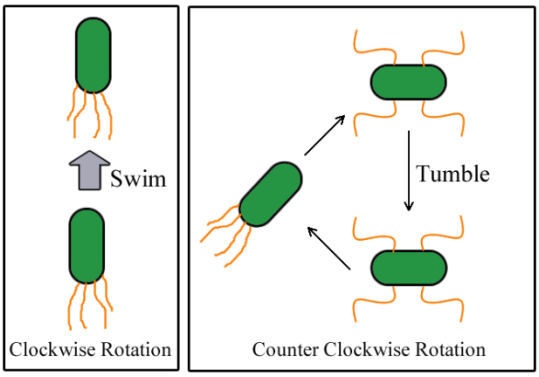



**Figure 5**- Swimming and rolling of E. coli bacterium

**2- Swarming:** E. coli bacteria exhibit a movement behavior among the bacteria for searching food during the chemotaxis stage. There is both pushing and pulling behavior among bacteria. E. coli bacteria produce movement information by secreting an aspartate to allow individual bacteria to travel to the center of the population and assemble them. At the same time, bacteria are kept at a certain distance according to the relevant pushing and pulling information. [20, 21].

**3- Reproduction:** After a while, bacteria with poor foraging ability are eliminated. Healthier bacteria with strong foraging ability will split in half producing offspring to maintain the population's size. Thus, the bacterial population is kept constant [20, 21].

**4- Elimination-Dispersal:** During the forging process, sudden or gradual environmental changes can occur. With these changes, some group of bacteria dies, while others migrate to new areas. The unexpected situations such as the death of bacteria or migration to new areas cannot be ruled out. The elimination-dispersal process has been proposed to control these situations. In this case, bacteria that die or migrate are replaced by randomly produced new substitute bacteria. [20, 21].

Realization of the BFO Algorithm;
Initial Values:
*P, N, nc, ns, nre, ned, Ped* and *S (i),*

*Here;*
*P* : *Search space dimension*
*N* : *Bacteria number in the population*
*nc* : *Chemotaxis steps number*
*ns* : *Swimming steps number*
*nre* : *Reproduction steps number*
*ned* : *Elimination-Dispersal steps number*
*S(i)* : *Step dimension*
$J_{cc}$ : *Objective function*
*Ped* : *Elimination-Dispersal steps probability*
$r^i(x,y,z)$ : *i th bacterium position vector*
*i = 1, 2,…, N.*
*F(i,x,y,z): Fitness function*

Initially, $x = y = z = 0$

**1-** *Elimination-Dispersal process: z = z +1*
**2-** Reproduction *process: y= y+1*
**3-** Chemotaxis *process*: *x= x*

**a.** For *i = 1,2,…..,N,*
Initialize the chemotactic step for bacteria i.

**b.** Find *F(i,x,y,z)*

$$F(i,x,y,z) = F(i,x,y,z) + F_{cc}(r^i(x,y,z), P(x,y,z)) \quad (7)$$

*Where;*

$$F_{cc}(r, P(x,y,z)) = \sum_{i=1}^{N} F_{cc}(r, r^i(x,y,z)) \quad (8)$$

**c.** Perform assignment $F_{last} = F(i,x,y,z)$ Keep this value until you get a better result through the swimming operation.

**d.** Rolling: With $\Delta m\ (i)$, $m = 1, 2, \ldots, p$
Generate a random vector $\Delta \in \mathfrak{R}^p(i)$
*p* in the range [-1, 1].

**e.** Move:

$$r^i(x+1,y,z) = r^i(x,y,z) + S(i)\frac{\Delta_i}{\sqrt{\Delta^T(i)\Delta(i)}} \quad (9)$$

Perform this formula.
For *i* th Bacteria, this result will be in *S(i)* step size and in the rolling direction.

**f.** Calculate *F(i,x+1,y,z)*

$$F(i,x+1,y,z) = F(i,x+1,y,z) + F_{cc}(r^i(x+1,y,z), P(x+1,y,z)) \quad (10)$$

**g.** Swimming:
*i) m = 0 (m: the swim length counter)*
*ii)* While *m < ns*;

- Perform assignment *m = m+1*
- If $F(i,x+1,y,z) < J_{last}$

$F_{last} = F(i,x+1,y,z)$

$$r^i(x+1,y,z) = r^i(x+1,y,z) + S(i)\frac{\Delta_i}{\sqrt{\Delta^T(i)\Delta(i)}} \quad (11)$$

*And* find the *F(i,x+1,y,z).*

- If *m = ns*, stop *m* for this bacteria.

ERKEN GÖRÜNÜM

**h.** If not the last bacteria *(i ≠ N)*, select the next bacterium. *(i = i + 1)* and go to step "b".

**4-** If $j < n_C$ Return step-3

**5-** Reproduction Process:

**a.** For *y*, *z* and *i = 1, 2, …, N* values:

$$j_{health} = \sum_{j=1}^{N_C+1} F(i,x,y,z) \qquad (12)$$

It is the function that expresses the healthy life cycle of a bacterium. In other words, it is the health status of bacteria i. Finally, rank the bacteria and their chemotactic parameters from smallest to largest according to the $J_{health}$ values obtained.

**b.** *Nr = N*/2 bacteria are considered dead. Their health condition is worse than others in the lower half of the ranking. In this case, *Nr* bacteria with better health status and remaining at the top of the ranking are produced by dividing. The each of new bacteria replaces dead bacteria.

**6-** If *y < nre*, *return* step-2.

Perform the chemotactic steps with the new produced bacteria.

**7-** Elimination-Dispersion:

*Eliminate and disperse all bacteria in the* $i = 1, 2, \ldots, N$ *array depending on the Ped.*

In this step, a bacterium simply moves from its current location to a new location. The population count remains constant during this step.

**8-** If *z < ned* return step-1, else end the program.

In this study, it was aimed to obtain the best location of E. Coli bacteria by minimizing the objective function (Fobj) for BFO. The objective function is formulated to find the best gain value. For this purpose, the NCC value was determined for the minimization process. After embedding watermarks to the original images, "gaussian", "shot", "salt & pepper" and "speckle" noises were added to the watermarked images, respectively. After adding noise, the watermark extraction process was performed and the NCC value between the extracted watermark and the original watermark was found. The inverse of the sum four calculated NCCs was determined as the objective function of the BFO.

$$F_{obj} = \frac{1}{NCC_1+NCC_2+NCC_3+NCC_4} \qquad (13)$$

Here;

NCC1 : NCC Value after adding first noise

NCC2 : NCC Value after adding second noise

NCC3 : NCC Value after adding third noise

NCC4 : NCC Value after adding fourth noise

**E- Particle Swarm Optimization**

PSO is an intuitive, stochastic and parallel method. This method firstly has been used to find optimal results for nonlinear numerical problems by modeling the bird, fish and insect flocks' movements. PSO is a population-based probabilistic optimization technique. it produces solutions to multi-parameter and multivariate optimization processes [19, 23, 24, 25].

PSO is proposed by Eberhart and Kennedy in 1995 [24]. The particle swarm concept has emerged as a simulation of a simplified social system. The initial aim was to graphically simulate the behavior of flocks of birds or fish. However, it was discovered that the particle swarm model could be used as an optimization method after graphical simulation [23, 26].

Although bird communities do not know the location of the actual food source, they try to find out how far they are from the food source. Birds follow the closest bird to the food source to find out the distance to the food source. In the PSO, each bird is represented as a particle and the bird community is represented as a swarm. When the particle moves, the fitness value of its coordinates, that is, how far it is from the food, is calculated. A particle must know the coordinates in which the best fitness value has been obtained and its velocity in those coordinates. In the solution space, the velocity of the particles in each dimension and how their direction changes each time will be obtained from the combination of their neighbors' best coordinates and their own personal best coordinates. [19].

The benefits of the PSO algorithm are as follows: (1) It has excellent robustness. It can be adapted to different applications by making very minor changes. (2) It has a powerful and wide ability. The basis of the algorithm is based on an evolutionary continuum. Therefore, it can be easily used in parallel computation. (3) It can quickly converge to the optimization value. (4) Its performance can be increased by using it in a hybrid structure with other algorithms. [23].

In this paper, the PSO technique is used to set the best position of the chemotactic parameters in the BFO algorithm [27]. *To calculate PSO;*

$$v_i(t+1) = w \times v_i(t) + C_1 \times rand_1\left(Pbest_i(t) - x_i(t)\right) \times rand_2\left(Gbest_i(t) - x_i(t)\right) \qquad (14)$$

$$x_i(t+1) = x_i(t) + v_i(t+1) \qquad (15)$$

here;

*i* : *Particle Number*
*t* : *Number of Iterations*
*v* : *Particle Velocity*
*x* : *Particle location*
*rand* : *Random Function*
*Pbest* : *Best position visited by particle i*
*Gbest* : *Best position discovered*
*w* : *Positive inertia weight*
$C_1$ , $C_2$ : *Acceleration coefficients*

ERKEN GÖRÜNÜM

## III. WATERMARKING PROCESS

The flow chart of the watermarking process (Figure 6) has been drawn and the steps of the watermarking process have been performed as here;

**a)** The original image and the watermark image are decomposed four sub-bands (LL, LH, HL, HH) by DWT technique.

**b)** DCT is applied to both images after the high frequency sub-band HH is separated.

**c)** Adaptive scaling factor is found for the watermark image.

**d)** DCT is applied to the HH band.

**e)** SVD is applied to both images after DCT.

**f)** The watermark is embedded in the image.

**g)** IDWT (Invers DWT), IDCT (Invers DCT) and (Invers SVD) are applied and watermarked image is obtained.

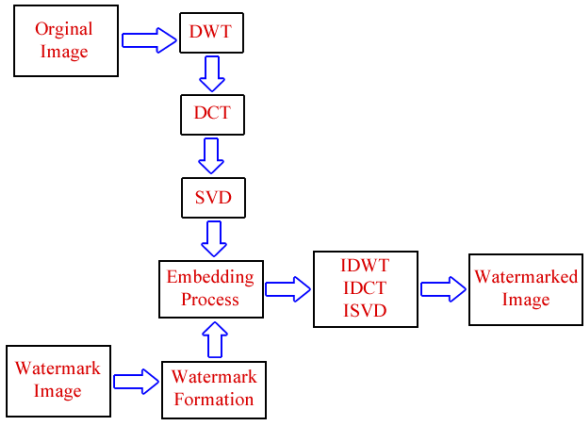



**Figure 6** – Watermarking algorithm flow chart

The flow chart of the watermark extraction process (Figure 7) has been designed and the watermark extraction steps have carried out as here;

**a)** Various noises are added to the watermarked image.

**b)** The original image and the watermarked image are decomposed four sub-bands with the DWT technique.

**c)** DCT is applied to both images after the high frequency sub-band HH is separated.

**d)** SVD is applied after DCT.

**e)** Optimization process is performed with BFO technique.

**f)** Watermark image is obtained by applying the watermark extraction process.

The hybrid structure has been practiced in five steps while embedding and extracting watermarks. In the first step, the processes have been carried out only with the DWT technique. In the second step, the hybrid structure of DWT and DCT technique has been used. In the third step, DWT, DCT and SVD have been used together. In the fourth step, the BFO technique has been added to the hybrid structure in the previous step and the processes have been repeated. In the last step, the PSO technique was added to the chemotactic step of the BFO technique and the processes in the fourth step have been repeated.

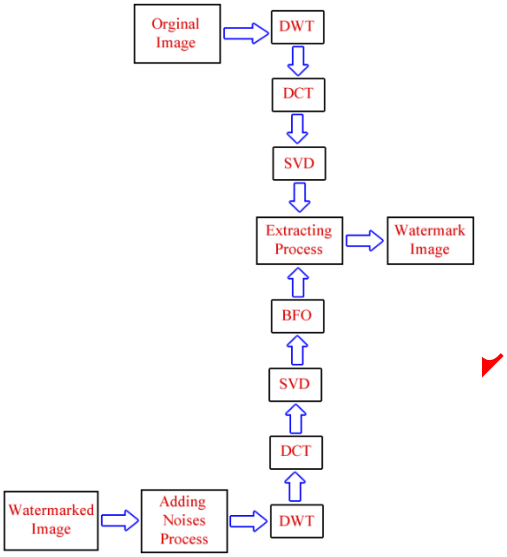



**Figure 7** – Flowchart of the watermark extraction algorithm

## IV. SECURITY TEST RESULTS USED TO COMPARE THE RESULTS OF WATERMARK APPLICATIONS

PSNR, NCC and IF values have been calculated to show the comparative performance of the applied algorithms.

*MSE*: Mean Square Error

$$MSE = \frac{1}{M \times N} \sum_{x=1}^{M} \sum_{y=1}^{N} [I(x,y) - I'(x,y)]^2 \qquad (16)$$

$$PSNR = 10\, log_{10}(\frac{255}{MSE}) \qquad (17)$$

Here;

*M* : *Width of Original Image*
*N* : *Original Image Height*
*I(x,y)* : *Pixels of the Original Image*
$I'(x,y)$ : *Pixels of the Watermark Image*

PSNR is between 30 and 50 dB for lossy images with a bit depth of 8 bits.

$$NCC = \frac{\sum_{i=1}^{m} \sum_{j=1}^{n} w(i,j) * w\prime(i,j)}{\sqrt{((\sum_{j=1}^{n} w(i,j))^2)} \sqrt{((\sum_{j=1}^{n} w\prime(i,j))^2)}} \qquad (18)$$

$w\,(i,j)$ : *Original Watermark*
$w'(i,j)$ : *Extracted watermark*
*m* : *Watermark Width*
*n* : *Watermark Height*

The *NCC* value is between 0 and 1. For two identical images, *NCC* value equal to 1 indicates perfect similarity between the two images [6].

The IF indicates the proximity of a watermarked image to the reference of the original image [28].

ERKEN CU

$$IF = 1 - \frac{\sum_{i=1}^{M}\sum_{j=1}^{N} I(i,j) * I\prime(i,j)}{\sum_{i=1}^{M}\sum_{j=1}^{N} I(i,j)^2} \quad (19)$$

Here;

*M* : *Width of Original Image*
*N* : *Original Image Height*
*I(x,y)* : *Pixels of the Original Image*
$I'(x,y)$ : *Pixels of the Watermark Image*

## V. EXPERIMANTAL RESULT

In this article, *512×512* pixel standard images named lena, cameraman, mandril, angiograph, spine, ctskull and fractal-iris were used for experimental studies. The *17×9* pixel image consisting of letters and numbers was used for the watermark. MATLAB R2020b program was used for experimental studies. In the experimental study, the following processes were applied to each of the seven Images named above, in order:

**Step 1:** The original image and the watermark image were decomposed four separate sub-bands with the DWT technique. The watermark embedding process was applied. Then the watermark image was obtained by applying the watermark extraction process.

**Step 2:** In this step, after the DWT process, DCT was applied to the original image and the watermark image and the watermark embedding process was applied. "Gaussian", "shot", "salt & pepper" and "speckle" noises were added to the watermarked picture, respectively. After the noise addition process, the watermark image was obtained by applying the watermark extraction process.

**Step 3:** The SVD technique was added to the process in the second step and the processes were repeated. Then, the watermark image was obtained with the watermark extraction process.

**Step 4:** The noise added picture in the third step was optimized using the BFO technique. The original image and the watermark image were re-extracted from the noise-added watermarked image.

**Step 5:** Fourth step was repeated using the PSO algorithm to set the best position of the chemotactic parameters in the BFO algorithm of the fourth step, and the original image and watermark image were extracted again.

*PSNR*, *NCC* and *IF* values have been recorded to see the comparative performance of the techniques and algorithms applied in each of these steps. These five steps have been applied separately for seven original images and the following results have been obtained.



**Figure 8** – Original Lena Image and Watermark Image

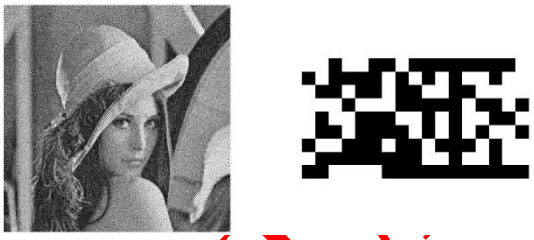


**Figure 9** – Watermarked Lena Image with DWT and Recovered Watermark From DWT



**Figure 10** – Watermarked Lena Image with DWT-DCT and Recovered Watermark From DWT-DCT

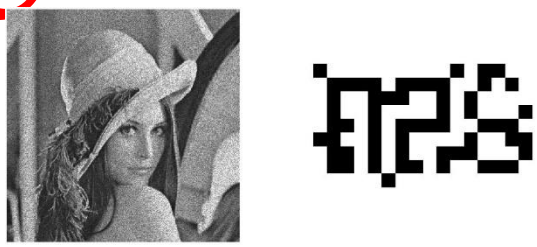


**Figure 11** – Watermarked Lena Image with DWT-DCT-SVD and Recovered Watermark From DWT-DCT-SVD

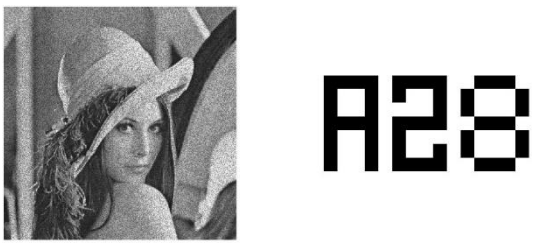


**Figure 12** – Watermarked Lena Image with DWT-DCT-SVD-BFO and Recovered Watermark From DWT-DCT-SVD-BFO

TRENGOVNO





**Figure 13** – Watermarked Lena Image with DWT-DCT-SVD-PBFO and Recovered Watermark From DWT-DCT-SVD-PBFO (BFO with PSO)

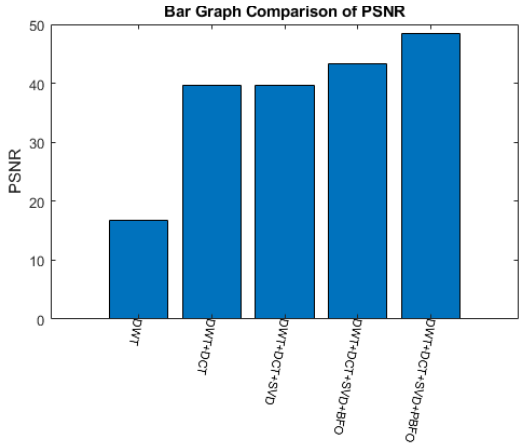



**Figure 14** - *PSNR* and *NCC* Bar Graph for Lena Image

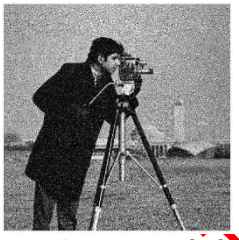
**Table 1**- Lena image performance values

| Method | Security Test Results | | |
|---|---|---|---|
| | *PSNR* | *NCC* | *IF* |
| DWT | 15.98 | 0.0017647 | -0.00036181 |
| DWT-DCT | 38.993 | 0.003451 | -0.0003558 |
| DWT-DCT-SVD | 38.92 | 0.0038824 | -0.00036181 |
| DWT-DCT-SVD-BFO | 42.651 | 0.0036863 | -0.00015327 |
| DWT-DCT-SVD-PBFO | 47.45 | 0.0034118 | -5.0754e-05 |





**Figure 15** – Original Cameraman Image and Watermark Image



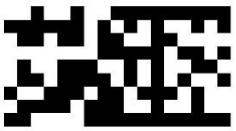


**Figure 16** – Watermarked Cameraman Image with DWT and Recovered Watermark From DWT





**Figure 17** – Watermarked Cameraman Image with DWT-DCT and Recovered Watermark From DWT-DCT



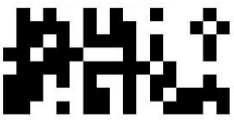


**Figure 18** – Watermarked Cameraman Image with DWT-DCT-SVD and Recovered Watermark From DWT-DCT-SVD



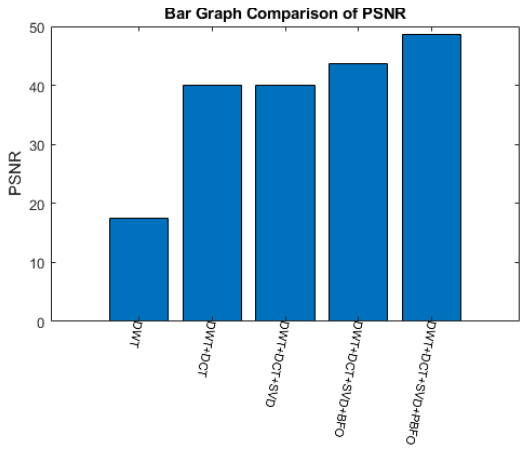


**Figure 19** – Watermarked Cameraman Image with DWT-DCT-SVD-BFO and Recovered Watermark From DWT-DCT-SVD-BFO





**Figure 20** – Watermarked Cameraman Image with DWT-DCT-SVD-PBFO and Recovered Watermark From DWT-DCT-SVD-PBFO



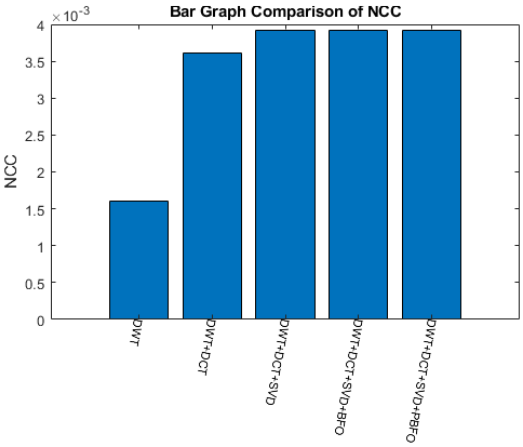




**Figure 21** - *PSNR* and *NCC* Bar Graph for Cameraman Image

**Table 2**- Cameraman image performance values

| Method | Security Test Results | | |
|---|---|---|---|
| | *PSNR* | *NCC* | *IF* |
| DWT | 18.009 | 0.0015294 | -0.00077215 |
| DWT-DCT | 40.115 | 0.0036078 | -0.00076232 |
| DWT-DCT-SVD | 40.059 | 0.0039216 | -0.00077215 |
| DWT-DCT-SVD-BFO | 43.783 | 0.0039216 | -0.00032757 |
| DWT-DCT-SVD-PBFO | 48.657 | 0.0038039 | -0.00010663 |

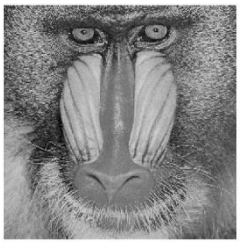
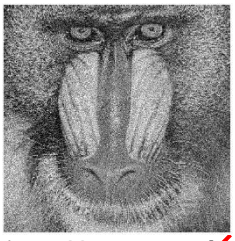




**Figure 22** – Original Mandril Image and Watermark Image



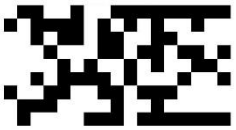


**Figure 23** – Watermarked Mandril Image with DWT and Recovered Watermark From DWT





**Figure 24** – Watermarked Mandril Image with DWT-DCT and Recovered Watermark From DWT-DCT

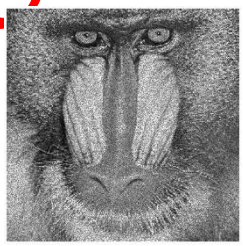




**Figure 25** – Watermarked Mandril Image with DWT-DCT-SVD and Recovered Watermark From DWT-DCT-SVD

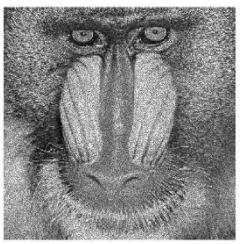




**Figure 26** – Watermarked Mandril Image with DWT-DCT-SVD-BFO and Recovered Watermark From DWT-DCT-SVD-BFO

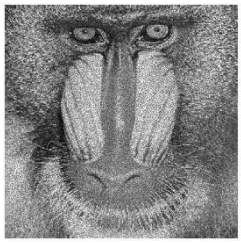




**Figure 27** – Watermarked Mandril Image with DWT-DCT-SVD-PBFO and Recovered Watermark From DWT-DCT-SVD-PBFO

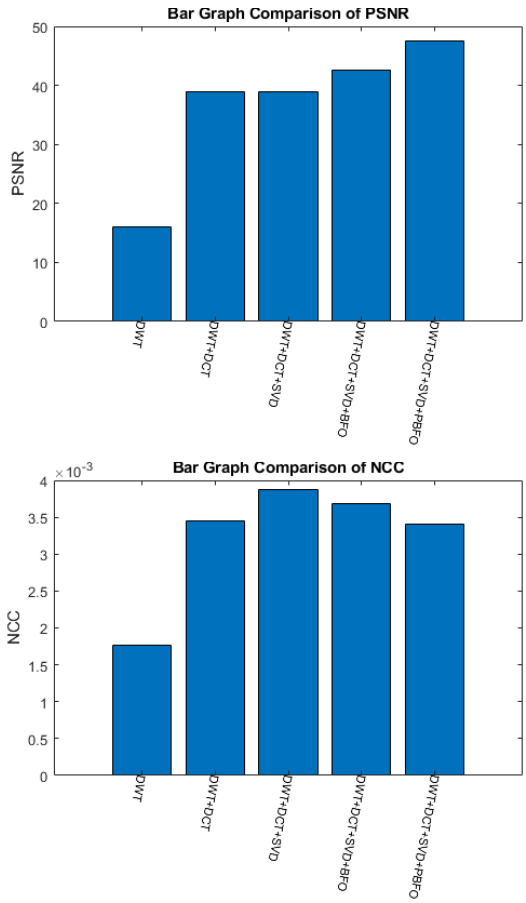



**Figure 28** - *PSNR* and *NCC* Bar Graph for Mandril Image

**Table 3**- Mandril image performance values

| Method | Security Test Results | | |
|---|---|---|---|
| | *PSNR* | *NCC* | *IF* |
| DWT | 17.11 | 0.0016471 | -0.0003373 |
| DWT-DCT | 40.048 | 0.0036078 | -0.00033378 |
| DWT-DCT-SVD | 40.002 | 0.0038824 | -0.0003373 |
| DWT-DCT-SVD-BFO | 43.696 | 0.0038431 | -0.00014409 |
| DWT-DCT-SVD-PBFO | 48.63 | 0.0037647 | -4.627e-05 |





**Figure 29** – Original Angiograph Image and Watermark Image



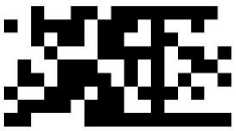


**Figure 30** – Watermarked Angiograph Image with DWT and Recovered Watermark From DWT

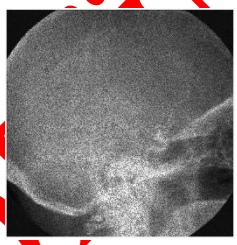




**Figure 31** – Watermarked Angiograph Image with DWT-DCT and Recovered Watermark From DWT-DCT





**Figure 32** – Watermarked Angiograph Image with DWT-DCT-SVD and Recovered Watermark From DWT-DCT-SVD

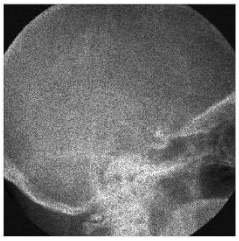




**Figure 33** – Watermarked Angiograph Image with DWT-DCT-SVD-BFO and Recovered Watermark From DWT-DCT-SVD-BFO

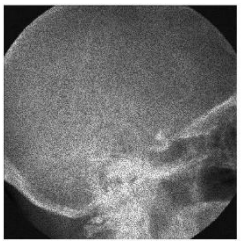
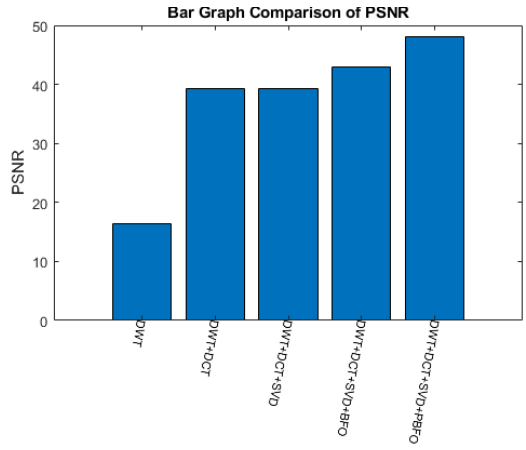



**Figure 34** – Watermarked Angiograph Image with DWT-DCT-SVD-PBFO and Recovered Watermark From DWT-DCT-SVD-PBFO



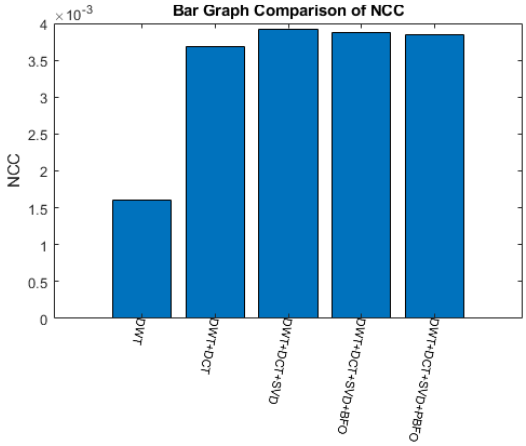




**Figure 35** - *PSNR* and *NCC* Bar Graph for Angiograph Image

**Table 4**- Angiograph image performance values

| Method | Security Test Results | | |
|---|---|---|---|
| | *PSNR* | *NCC* | *IF* |
| DWT | 16.771 | 0.0015686 | -0.00036983 |
| DWT-DCT | 39.694 | 0.0038824 | -0.0003643 |
| DWT-DCT-SVD | 39.629 | 0.0039216 | -0.00036983 |
| DWT-DCT-SVD-BFO | 43.313 | 0.0039216 | -0.00015833 |
| DWT-DCT-SVD-PBFO | 48.46 | 0.0038431 | -4.8399e-05 |




**Figure 36** – Original Spine Image and Watermark Image

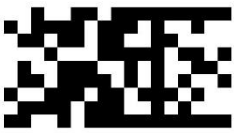



**Figure 37** – Watermarked Spine Image with DWT and Recovered Watermark From DWT




**Figure 38** – Watermarked Spine Image with DWT-DCT and Recovered Watermark From DWT-DCT




**Figure 39** – Watermarked Spine Image with DWT-DCT-SVD and Recovered Watermark From DWT-DCT-SVD




**Figure 40** – Watermarked Spine Image with DWT-DCT-SVD-BFO and Recovered Watermark From DWT-DCT-SVD-BFO




**Figure 41** – Watermarked Spine Image with DWT-DCT-SVD-PBFO and Recovered Watermark From DWT-DCT-SVD-PBFO

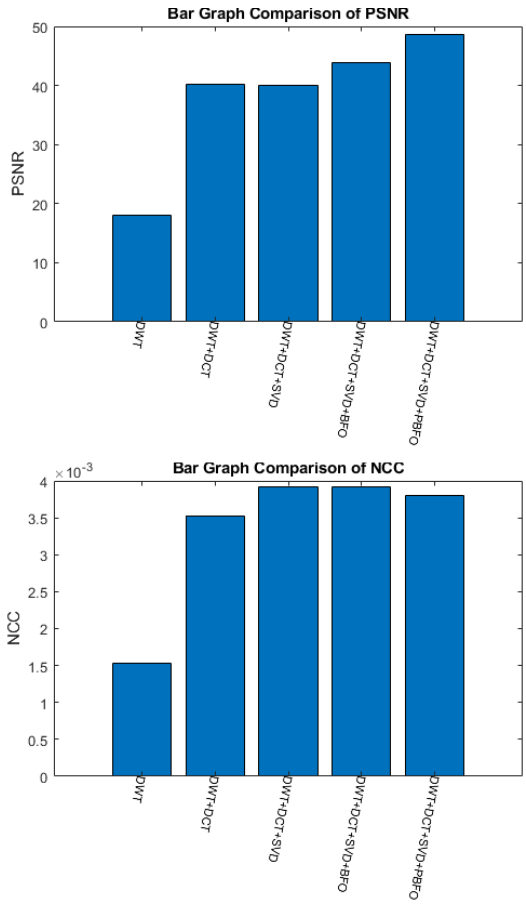



**Figure 42** – *PSNR* and *NCC* Bar Graph for Spine Image

**Table 5**: Spine image performance values

| Method | Security Test Results | | |
|---|---|---|---|
| | *PSNR* | *NCC* | *IF* |
| DWT | 17.788 | 0.0016078 | -0.00020208 |
| DWT-DCT | 39.87 | 0.0035686 | -0.00019906 |
| DWT-DCT-SVD | 39.804 | 0.0038824 | -0.00020208 |
| DWT-DCT-SVD-BFO | 43.492 | 0.0038039 | -8.6455e-05 |
| DWT-DCT-SVD-PBFO | 48.4 | 0.0037255 | -2.7926e-05 |




**Figure 43** – Original Ctskull Image and Watermark Image

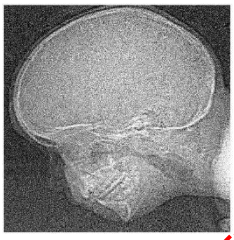
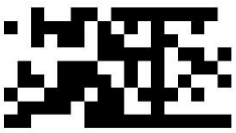



**Figure 44** – Watermarked Ctskull Image with DWT and Recovered Watermark From DWT




**Figure 45** – Watermarked Ctskull Image with DWT-DCT and Recovered Watermark From DWT-DCT

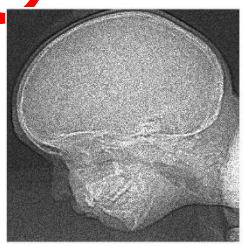



**Figure 46** – Watermarked Ctskull Image with DWT-DCT-SVD and Recovered Watermark From DWT-DCT-SVD

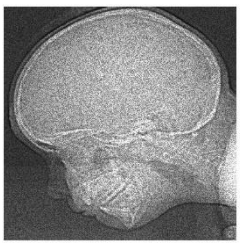



**Figure 47** – Watermarked Ctskull Image with DWT-DCT-SVD-BFO and Recovered Watermark From DWT-DCT-SVD-BFO

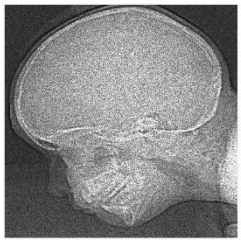
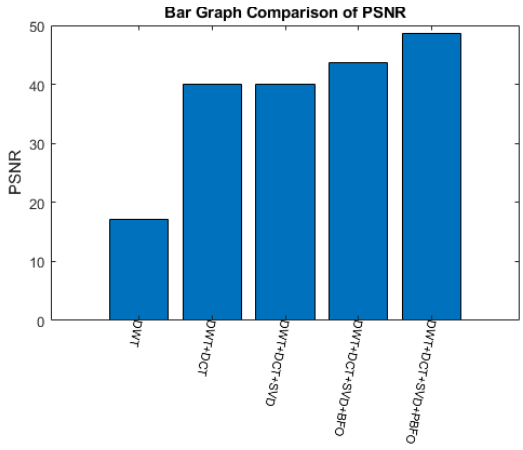




**Figure 48** – Watermarked Ctskull Image with DWT-DCT-SVD-PBFO and Recovered Watermark From DWT-DCT-SVD-PBFO



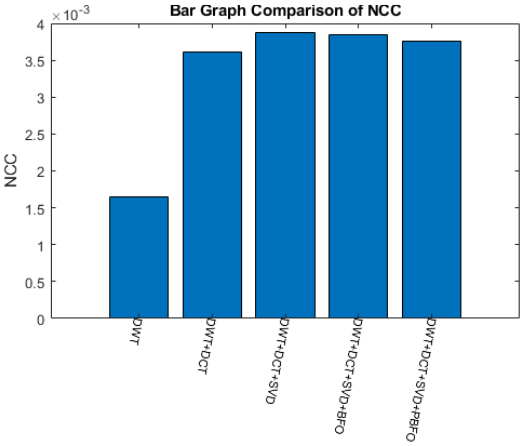




**Figure 49** - *PSNR* and *NCC* Bar Graph for Ctskull Image

**Table 6**- Ctskull image performance values

| Method | Security Test Results | | |
|---|---|---|---|
| | *PSNR* | *NCC* | *IF* |
| DWT | 16.424 | 0.0016078 | -0.0005096 |
| DWT-DCT | 39.295 | 0.0036863 | -0.00050203 |
| DWT-DCT-SVD | 39.23 | 0.0039216 | -0.0005096 |
| DWT-DCT-SVD-BFO | 42.964 | 0.0038824 | -0.00021571 |
| DWT-DCT-SVD-PBFO | 48.006 | 0.0038431 | -6.7547e-05 |

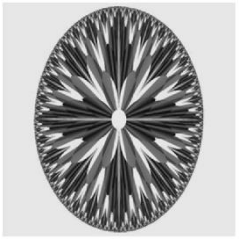
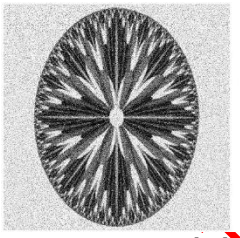




**Figure 50** – Original Fractal-iris Image and Watermark Image



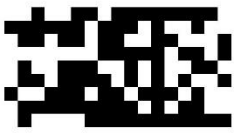
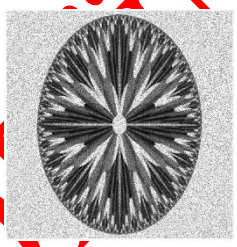


**Figure 51** – Watermarked Fractal-iris Image with DWT and Recovered Watermark From DWT



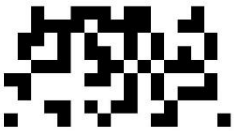
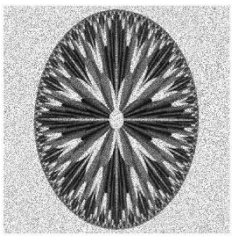


**Figure 52** – Watermarked Fractal-iris Image with DWT-DCT and Recovered Watermark From DWT-DCT



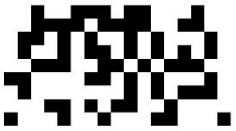


**Figure 53** – Watermarked Fractal-iris Image with DWT-DCT-SVD and Recovered Watermark From DWT-DCT-SVD

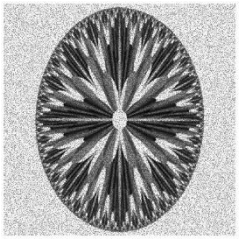




**Figure 54** – Watermarked Fractal-iris Image with DWT-DCT-SVD-BFO and Recovered Watermark From DWT-DCT-SVD-BFO

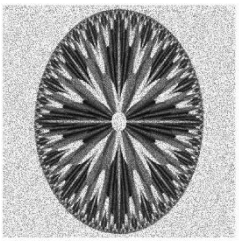
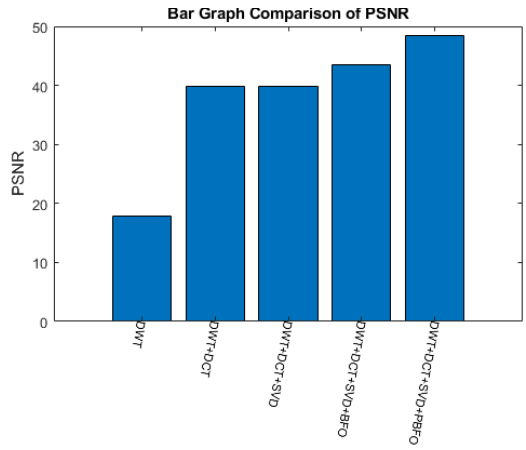


**Figure 55** – Watermarked Fractal-iris Image with DWT-DCT-SVD-PBFO and Recovered Watermark From DWT-DCT-SVD-PBFO



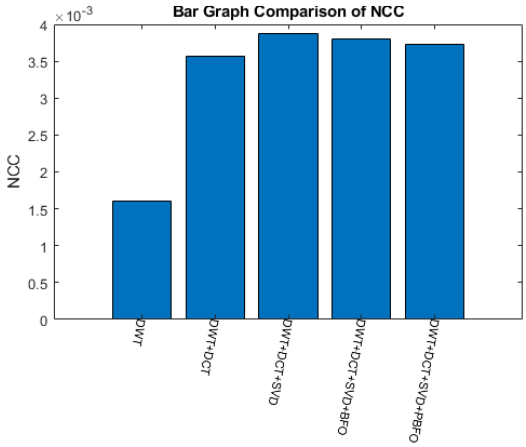




**Figure 56** - *PSNR* and *NCC* Bar Graph for Fractal-iris Image

**Table 7**- Fractal-iris image performance values

| Method | Security Test Results | | |
|---|---|---|---|
| | *PSNR* | *NCC* | *IF* |
| DWT | 17.427 | 0.0016078 | -0.00036549 |
| DWT-DCT | 40.044 | 0.0036078 | -0.00036074 |
| DWT-DCT-SVD | 39.988 | 0.0039216 | -0.00036549 |
| DWT-DCT-SVD-BFO | 43.709 | 0.0039216 | -0.00015513 |
| DWT-DCT-SVD-PBFO | 48.599 | 0.0039216 | -5.0322e-05 |

When the image performance tables are analyzed, it is seen that the applied techniques of hybrid watermarking and optimization give successful results, although there are slight differences in PSNR, NCC and IF values. It is seen that the extracted watermarks are understandable after step-by-step hybrid watermark techniques and optimization techniques. When the graphs are studied, PSNR values increase within acceptable limits and NCC values approach 1. When the IF values are studied, it is seen that the similarity between the original image and the watermarked image has increased.

PSNR is between 30 and 50 dB for lossy images with a bit depth of 8 bits. The accepted *PSNR* value approaches 50 dB. So, the result of our method was compared with other studies in the literature [1, 10, 14, 28, 29, 30, 31, 32, 33] in terms of mean average PSNR, as seen in Table 8. The success of the applied method was visualized by creating a bar graph of the values in Table 8 (Figure 57).

**Table 8** - The comparison of our method with the other methods in the literature according to the PSNR value

| METHOD | PSNR Values |
|---|---|
| Proposed Method | 48,31457 |
| Methods [28] | 46,24 |
| Methods [29] | 45,93 |
| Methods [30] | 45,4666 |
| Methods [31] | 44,12 |
| Methods [32] | 44,0567 |
| Methods [15] | 43,9351 |
| Methods [1] | 42,96 |
| Methods [33] | 41,3901 |
| Methods [10] | 38,2477 |

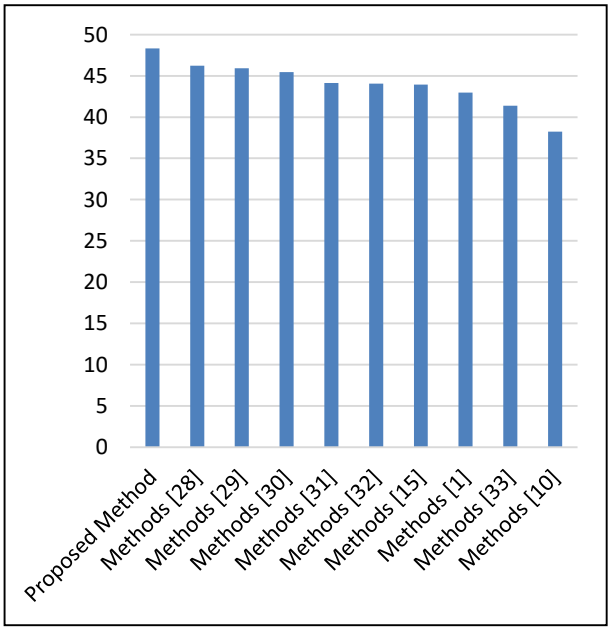



**Figure 57** – The average PSNR values comparison

JOURNAL

## VI. CONCLUSION

In this article, a hybrid watermarking method was applied by using DWT, DCT and SVD, which are among the watermarking methods used to prevent copyright violations and privacy violations in digital images. “Gaussian”, “shot”, “salt & pepper” and “speckle” noises were added to the watermarked image, respectively, and watermark extraction was performed from this noisy image. The watermark extraction was performed using the BFO algorithm in order to increase the success of this process. This step was repeated using the PSO to set the best position of the chemotatic parameters in the BFO algorithm. When the experimental results of PSNR, NCC and IF values are analyzed, it is obtained that the applied techniques are successful. As *PSNR* values go from the first stage of the application to the last stage, it is obtained that the accepted *PSNR* value approaches 50 dB. It is seen that the *NCC* value moves away from the zero value. When the *IF* values are analyze, it has been observed that the picture quality of the original picture increased as we go from the first stage of the application to the last stage. It has been observed that the applied hybrid structure and optimization techniques give successful results in embedding and extraction watermarks.

## DECLARATION OF ETHICAL STANDARDS

The authors of this article declare that the materials and methods used in this study do not require ethical committee permission and/or legal-special permission.

## AUTHORS’ CONTRIBUTIONS

**Sadık YILDIZ:** He conceptualized this study, created the methodology of the paper, performed the experiments and analyzed the results, and wrote the paper.

**Furkan ÜSTÜNSOY:** He conceptualized this study, created the methodology of the paper, performed the experiments and analyzed the results, and wrote the paper.

**Hasan Hüseyin SAYAN:** He conceptualized this study, created the methodology of the paper, performed the experiments and analyzed the results, and wrote the paper.

## CONFLICT OF INTEREST

There is no conflict of interest in this study.

## REFERENCES


[1] Al-maweri, N. A. S., Wan Adnan, W. A., Ramli, A. R., Samsudin, K., and Syed Ahmad, S., M., “A hybrid digital image watermarking algorithm based on DCT-DWT and auto-thresholding.”, Security Comm. Networks, 8: 4373–4395, (2015).

[2] K.A. Al-Afandy, E.M. EL-Rabaie, F.E.A. El-Samie, O.S. Faragallah, A. ELmhalaway, A.M. Shehata,"A Comparative Study For Color Systems Used In The DCT-DWT Watermarking Algorithm", ***Advances in Science, Technology and Engineering Systems Journal***, vol. 1, no. 5, pp. 42-49 (2016).

[3] Mishra A., Agarwal C., Sharma A., Bedi P., "Optimized gray-scale image watermarking using DWT–SVD and Firefly Algorithm", ***Expert Systems with Applications***, Volume 41, Issue 17, Pages 7858-7867, (2014).

[4] Golshan F., Mohammadi K., “A hybrid intelligent SVD-based perceptual shaping of a digital image watermark in DCT and DWT domain”, ***The Imaging Science Journal***, 61:1, 35-46, (2013).

[5] Mehto A., Mehra N., "Adaptive Lossless Medical Image Watermarking Algorithm Based on DCT & DWT", ***Procedia Computer Science***, Volume 78, Pages 88-94, (2016).

[6] Sharma S., Chauhan U., Khanam R., Singh K., "Digital Watermarking using Grasshopper Optimization Algorithm", ***Open Computer Science***, vol. 11, no. 1, pp. 330-336, (2021).

[7] Bose A., Maity S. P., "Secure sparse watermarking on DWT-SVD for digital images", ***Journal of Information Security and Applications***, Volume 68, 103255, (2022).

[8] Abdulrahman A. K., Öztürk S., "Çoklu Görüntü Damgalama Yönteminde Farklı Frekans Bölgelerinin Değerlendirilmesi", ***Bilişim Teknolojileri Dergisi***, c. 11, sayı 1, ss. 75-88, (2018).

[9] Bakwad K. M., Pattnaik S.S., Sohi B. S., Devi S., Panigrahi B. K. , Gollapudi S. V. R. S., “Bacterial Foraging Optimization Technique Cascaded with Adaptive Filter to Enhance Peak Signal to Noise Ratio from Single Image”, ***IETE Journal of Research***, 55:4, 173-179,(2009).

[10] Liu J., Huang J., Luo Y., Cao L., Yang S., Wei D., Zhou R., "An Optimized Image Watermarking Method Based on HD and SVD in DWT Domain", ***IEEE Access***, vol. 7, pp. 80849-80860, (2019).

[11] Kadian P., Arora N., Arora S. M., "Performance Evaluation of Robust Watermarking Using DWT-SVD and RDWT-SVD," ***6th International Conference on Signal Processing and Integrated Networks (SPIN)***, pp. 987-991, (2019).

[12] E. Elbaşı, " Two Bands Wavelet Based Robust Semi-Blind Image Watermarking", ***Politeknik Dergisi,*** 11(4): 329-337, (2008).

[13] Vishwakarma V. P., Dalal S., Sisaudia V., "Efficient Feature Extraction using DWT-DCT for Robust Face Recognition under varying Illuminations," ***2nd IEEE International Conference on Power Electronics, Intelligent Control and Energy Systems (ICPEICES)***, pp. 982-987, (2018).

[14] Wang M., Jiang H., Li Y., "Face recognition based on DWT/DCT and SVM", ***International Conference on Computer Application and System Modeling (ICCASM)***, pp. V3-507-V3-510, (2010).

[15] S. R. Sheriff, "Digital Image Watermarking using Singular Value Decomposition", ***AL-Rafidain Journal of Computer Sciences and Mathematics***, 7, 3, p-p 187-200, (2010).

[16] Dirckx S., Huybrechs D., Ongenae R., “On the computation of the SVD of Fourier submatrices”, ***arXiv:2208.12583v1*** **(math.NA),** (2022).

[17] Ahmadi S.B.B., Zhang G., Wei S., “Robust and hybrid SVD-based image watermarking schemes:” Multimed Tools Appl 79, 1075–1117, (2020).

[18] Mathew K D., “SVD based Image Watermarking Scheme”, ***IJCA Special Issue on Evolutionary***


ERKEN GÖRÜNÜM

***Computation for Optimization Techniques-ECOT***, pp. 21-24, (2010).

[19] Akyol S., Alataş B., "Güncel Sürü Zekası Optamizasyon Algoritmaları", ***Nevşehir Üniversitesi Fen Bilimleri Enstitüsü Dergisi***, c. 1, sayı. 1, ss. 0-0, (2012).

[20] Das, S., Biswas, A., Dasgupta, S., Abraham, A., "Bacterial Foraging Optimization Algorithm: Theoretical Foundations, Analysis, and Applications", ***Foundations of Computational Intelligence***, Volume 3, pp 23–55, (2009).

[21] Zhang Q., Chen, H., Luo J., Xu Y., Wu C., Li C., "Chaos Enhanced Bacterial Foraging Optimization for Global Optimization", ***in IEEE Access***, vol. 6, pp. 64905-64919, 2018.

[22] Bolat B., Altun O., Cortes P., Yıldız Y. E., Topal A. O., "A Comparison of Metaheuristics for the Allocation of Elevators to Calls in Buildings", ***Politeknik Dergisi***, 20(3): 519-52, (2017).

[23] Wang, D., Tan, D., Liu, L., "Particle swarm optimization algorithm: an overview", ***Soft Comput 22***, 387–408 (2018).

[24] Akyol K., Feneaker S. O. F., "Kaynaklı Kiriş Tasarımı Mühendislik Problemi İçin Kaotik Çoklu-sürü Parçacık Sürü Optimizasyonu", ***Politeknik Dergisi***, 1-1, (2022).

[25] Donuk K., Arı A., Özdemir M. F., "Hanbay D. Deep Feature Selection for Facial Emotion Recognition Based on BPSO and SVM", ***Politeknik Dergisi***, 1-1, (2022).

[26] Bharati S., Rahman M. A., Mandal S., Podder P., "Analysis of DWT, DCT, BFO & PBFO Algorithm for the Purpose of Medical Image Watermarking", ***International Conference on Innovation in Engineering and Technology (ICIET)***, pp. 1-6, (2018).

[27] Yousefi M., Omid M., Rafiee Sh., Ghaderi S.F., "Strategic planning for minimizing CO2 emissions using LP model based on forecasted energy demand by PSO Algorithm and ANN", ***International Journal Of Energy And Environment***, Volume 4, Issue 6, pp.1041-1052,(2013).

[28] Aliwa M. B., El-Tobely T. A., Fahmy M. M., Nasr M. S., Aziz M. H., "Fidelity and Robust Digital Watermarking Adaptively Pixel based on Medial Pyramid of Embedding Error Gray Scale Images", ***IJCSNS International Journal of Computer Science and Network Security***, Vol. 10 No. 6, pp. 284-314, (2010).

[29] Singh P., Devi K. J., Thakkar H. K., Kotecha K., "Region-Based Hybrid Medical Image Watermarking Scheme for Robust and Secured Transmission in IoMT,", IEEE Access, vol. 10, pp. 8974-8993, (2022).

[30] Thakkar, F.N., Srivastava, V.K., "A blind medical image watermarking: DWT-SVD based robust and secure approach for telemedicine applications". ***Multimed Tools Appl,*** 76, 3669–3697, (2017).

[31] Rajan B. K., Harshan H. M., Venugopal G., "Veterinary Image Enhancement using DWTDCT and Singular Value Decomposition," ***2020 International Conference on Communication and Signal Processing (ICCSP)***, pp. 0920-0924, (2020).

[32] Alzahrani A., Memon N. A., "Blind and Robust Watermarking Scheme in Hybrid Domain for Copyright Protection of Medical Images,", IEEE Access, vol. 9, pp. 113714-113734, (2021).

[33] Ma J., ChenJ., Wu G., "Robust Watermarking via Multidomain Transform Over Wireless Channel: Design and Experimental Validation,", IEEE Access, vol. 10, pp. 92284-92293, (2022).

BASIM ÖNCESİ GÖRÜNÜM